Heat transfer coefficient and skin friction determination of thermal radiation effects on MHD convective flow of alumina nanofluid through a non-Darcian porous plate

[1] **Ngiangia, A. T,** [2] **Orukari, M. A,**
[1] Department of Physics, University of Port Harcourt, P M B 5323 Choba, Port Harcourt, Nigeria
[2] Department of Mathematics and Computer Science, Niger Delta University, Wilberforce Island, Nigeria

Abstract
This work, analyzes the effect of thermal radiation on MHD alumina nanofluid through a non-Darcian porous medium. A Homotopy Pertubation Method (HPM) is employed to determine the temperature and velocity profiles of the nanofluid in order to consider the skin friction, heat transfer coefficient and other parameters that influenced the fluid. Using numerical computations, it is observed that increase in the Prandtl number (Pr), heat source term (Q > 0), magnetic Hartmann number (Ha), Porosity term (χ) and Grashof number (Gr) showed a decrease in the skin friction at the wall of the plate while increase in Reynolds number (Re), heat sink term (Q < 0) and radiation term (N) result in an increase in the skin friction. The Nusselt number increases as a result of increase in Prandtl number, radiation term, heat source term and nanoparticle volume fractions (ϕ) where as a decrease is observed with heat sink term. The temperature and velocity profiles were enhanced as a result of increasing heat sink term while a decrease is observed with increase in nanoparticle volume fractions, radiation, Prandtl number and heat source term. The velocity profile is enhanced as the Reynolds number is increased and diminished as the magnetic field intensity becomes stronger and non-Darcian term increases.

Keywords: Nusselt number; Alumina nanofluid, Skin friction; Porous plate, Homotopy Perturbation Method

Introduction
Heat transfer is the transport of heat from one point to another. Energy transfer in the form of heat due to convection is potent in several physical situations. Convection is of three types, namely, free convection, forced convection and mixed convection. Convection induced by buoyancy is termed free convection while forced convection is caused by external pressure gradient or object motion. A combination of the occurrence

of free and forced convection to heat transfer is mixed convection and readily realized in the flow of fluid in a channel. The effect of radiation on electrically conducting nanofluid has become industrially important and therefore cannot be overemphasized. It is pertinent therefore that the consideration of the effect of magnetic field is desirable. Several metallurgical and engineering processes occur at high temperatures and this explains the reason knowledge of radiation heat transfer on improved thermal conductivity fluid is important. In the work of Eckert and Drake [1], nuclear power plants, gas turbines, missiles and satellites and various propulsion devices for aircraft are some examples which require high temperatures and also require rapid heat transfer. According to Raisinghania [2], the skin friction at the walls of the channel is of practical importance because its mean value at the ends of the walls is employed to estimate the energy losses in channels. As a result of the need for rapid heat transfer fluid more than the conductivity of water, nanofluids are vigorously studied for a possible replacement of base fluid (water) or at best complement it. In simple terms, nanofluid is obtained when a measured quantity of nanoparticles is mixed with a given volume of base fluid. Solid nanoparticles, has sizes range between 1nm – 100nm. Laminar flow of fluids through porous media, started with Darcy but Darcy's law is valid only for slow flows through porous media with low permeability. At higher flow rates, there is a departure from linear law and inertia effects become important. It is in the light of the possible turbulent flow that the effect becomes non-Darcian. Heat transfer performance is a better indicator than the heat conductivity ratio of nanofluids. As a result, modeling of nanofluid heat transfer coefficients and skin frictions are gaining attention from researchers. Studies such as Maiga et al [3,4], Roy et al [5], Wang et al [6], Khannafer et al [7], Xuan and Roetzel [8] and Abu-nada et al [9], considered primarily the convective heat transfer characteristics of nanofluids and concluded that the average Nusselt number got enhanced with the increase in volume fractions of nanoparticles and thermal Grashof number. Further, Polidori et al [10] and Mansour et al [11], investigated the natural convection of heat transfer of a mixture of alumina nanoparticles with water, and not forgetting that an accurate established theory to predict the heat transfer characteristics of nanofluid is difficult. The aim is an attempt to using the hydrodynamic equations of motion to predict the enhancement of or otherwise of heat transfer coefficient and skin friction on the effect of radiation and magnetic field in mixture of alumina nanoparticles in water to form alumina nanofluid. The results shall be compared with the works of Polidori et al [10] and Mansour et al [11], and deductions made.

Preliminaries of Homotopy perturbation method

To illustrate the essential steps to be followed in the application of Homotopy Perturbation Method (HPM), a nonlinear differential equation of the form

$$\Theta(z) - \varpi(r) = 0 \qquad r \in \Omega \tag{1}$$

and imposing the boundary conditions

$$\Xi\left(z, \frac{\partial z}{\partial r}\right) = 0 \qquad r \in \Gamma \tag{2}$$

is assumed. Θ is differential operator, Ξ is boundary operator, $\varpi(r)$ is known analytical function and Γ is the boundary of the domain Ω. The operator Θ can be divided into two parts, L and N, where
L is linear and N is nonlinear. Eq.(1) can therefore be written as:

$$L(z) + N(z) - \varpi(r) = 0 \qquad r \in \Omega \qquad (3)$$

To apply the Homotopy perturbation techniques, a construction of Homotopy given as

$\wp(r, p): \Omega \times [0,1] \to \Re$ that satisfies

$$H(\wp, p) = (1-p)[L(\wp) - N(z_0)] + p[\Theta(\wp) - \varpi(z)] = 0 \qquad (4)$$

In Eq. (4), $p \in [0,1]$ is an embedding parameter, while z_0 is an initial approximation of Eq. (1), which satisfies the boundary conditions. We can assume that the solution of Eq. (4) can be written as a power series in p :

$$\wp = \wp_0 + p\wp_1 + p^2\wp_2 + ... \qquad (5)$$

and the approximation is stated as

$$z = \lim_{p \to 1} \wp = \wp_0 + \wp_1 + \wp_2 + ... \qquad (6)$$

The combination of the perturbation method and the homotopy method is called the HPM, which eliminates the limitations of the traditional perturbation methods while keeping all its advantages. The series (Eq.6) is convergent for most cases. However, the convergent rate depends on the nonlinear operator $\Theta(\wp)$. However, He [12] made the following suggestions:
(i). the second derivative of $N(\wp)$ must be small because the parameter may be relatively large, $p \to 1$
(ii). the norm of $L^{-1}\dfrac{\partial N}{\partial \wp}$ must be < 1 so that the series converges.

Formalism
We consider an unsteady two dimensional boundary layer flow of viscous, oscillatory, incompressible, radiating nanofluid along a semi-infinite flat vertical plate in the presence of thermal and concentration buoyancy effects. The $x' -$axis is taken along the vertical infinite plate in the upward direction and the $y' -$axis normal to the plate. The effect of induced magnetic field is neglected on the assumption that it is minimal. Using the Boussinesq's approximation, the governing equations of the nanofluid flow are given as

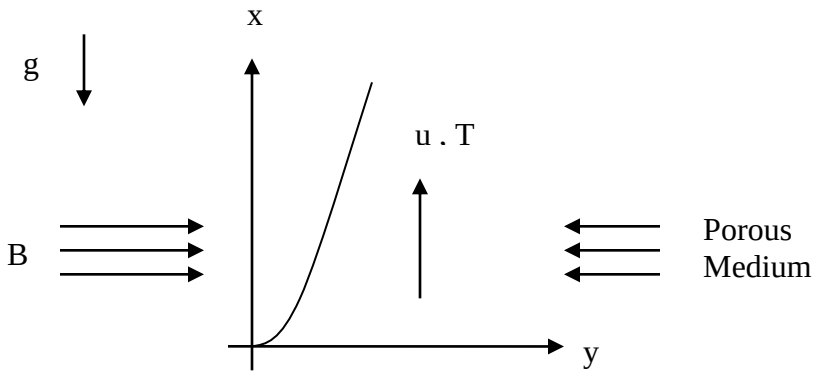

Fig. 1: Physical model and coordinate system of the problem

$$\frac{\partial u'}{\partial x'}+\frac{\partial v'}{\partial y'}=0 \tag{7}$$

$$\frac{\partial u'}{\partial t'}+u'\frac{\partial u'}{\partial x'}+v'\frac{\partial u'}{\partial y'}=\frac{\mu_{nf}}{\rho_{nf}}\left(\frac{\partial^2 u}{\partial x'^2}+\frac{\partial^2 u}{\partial y'^2}\right)-\frac{\sigma B_0^2 u'}{\rho_{nf}}-\frac{\nu u'}{\rho_{nf}\kappa}+g\beta_{nf}\left(T-T_\infty\right) \tag{8}$$

$$\frac{\partial T}{\partial t'}+\left(u'\frac{\partial T}{\partial x'}+v'\frac{\partial T}{\partial y'}\right)=\frac{k_{nf}}{\left(\rho C_p\right)_{nf}}\left(\frac{\partial^2 T}{\partial x'^2}+\frac{\partial^2 T}{\partial y'^2}\right)-\frac{1}{\left(\rho C_p\right)_{nf}}\left(\frac{\partial q_r}{\partial x'}+\frac{\partial q_r}{\partial y'}\right)-\frac{Q_0\left(T-T_\infty\right)}{\left(\rho C_p\right)_{nf}} \tag{9}$$

Subject to the boundary conditions (Karthikeyan et al,[13])

$$u'=u_0 \quad T=T+\varphi\left(T-T_\infty\right) \quad \text{at } y=0 \tag{10}$$

$$u'\to 0,\ T\to T_\infty \text{ as } y'\to\infty$$

where u' and v' are velocities in x' and y' directions respectively, t' is time, ρ_{nf} is density of nanofluid, μ_{nf} is dynamic viscosity of nanofluid, σ is electrical conductivity of base fluid, B is imposed magnetic induction, g is acceleration due to gravity, β_{nf} is

thermal expansion due to temperature, Q_0 is heat function, T is temperature of nanofluid, T_∞ is free stream temperature,, k_{nf} is thermal conductivity of nanofluid, $(C_p)_{nf}$ is specific heat at constant pressure, q_r is radiation term,

In the work of Batchelor [14] and Bhattacharya et al [15], ratio of dynamic viscosity and ratio of thermal conductivity which are valid for spherical and non spherical shapes nanoparticles are defined respectively as

$$\frac{\mu_{nf}}{\mu_f} = \left(1 + 2.5\phi + 6.2\phi^2\right) \tag{11}$$

$$\frac{k_{nf}}{k_f} = \phi\frac{k_s}{k_f} + (1-\phi) \tag{12}$$

where k_s is the thermal conductivity of nanoparticles and k_f is the thermal conductivity of base fluid.

According to the work of Tiwari and Das [16] and Asma et al [17], density of nanofluid (ρ_{nf}), thermal expansion due to temperature of nanofluid (β_{nf}), specific heat at constant pressure of nanofluid $(C_p)_{nf}$ are respectively

$$\begin{aligned}\rho_{nf} &= (1-\phi)\rho_f + \phi\rho_s \\ \beta_{nf} &= (1-\phi)\beta_f + \phi\beta_s \\ (C_p)_{nf} &= (1-\phi)(C_p)_f + \phi(C_p)_s\end{aligned} \tag{13}$$

where k_B is the Stefan-Boltzmann constant, ϕ is the nanoparticles volume fractions, ρ_f and ρ_s are the densities of the base fluid and solid nanoparticles, β_f and β_s are the thermal expansion due to temperature of base fluid and solid nanoparticles and $(C_p)_f$ and $(C_p)_s$ are the specific heat at constant pressure due to base fluid and solid nanoparticles. The thermo physical properties of alumina (Al_2O_3) nanoparticles and water (H_2O) as base fluid are presented in **Table 1.**

Table 1: Thermo-physical properties of water and alumina (Aaiza et al [18]).

Property	Water	Alumina
Specific heat $C_p\left(Jkg^{-1}K^{-1}\right)$	4179	765
Density $\rho\left(kgm^{-3}\right)$	997.1	3970
Thermal conductivity $k\left(Wm^{-1}K^{-1}\right)$	0.6	40
Thermal expansion $\beta\times10^{-5}\left(K^{-1}\right)$	21	0.85

In order to consider the effect of radiation on an optically thick model in which the thermal layer becomes very thick or highly absorbing as described by Rosseland approximation, Cogley et al [19] stated it as

$$\frac{\partial q_r}{\partial y} = -\frac{4k_B}{3\alpha}\frac{\partial T^4}{\partial y} \tag{14}$$

where α is the absorption coefficient. If temperature difference within the flow of the nanofluid is sufficiently small, we can approximate T^4 using Taylor series expansion about T_∞ and neglect higher order terms, the expression results into

$$T^4 = 4T_\infty^3 T - 3T_\infty^4 \tag{15}$$

Dimensional Analysis

Dimensional homogeneity of the governing nanofluid equations using the Buckingham-π – theorem is stated as

$$u = \frac{u'}{v'}, y = \frac{y'}{x'}, t = \frac{t'u'}{x'}, \mathrm{Re}^{-1} = \frac{\mu_{nf}\rho_f}{\rho_{nf}\mu_f}, \theta = \frac{T - T_0}{T_0}, \mathrm{Pr} = \frac{k_f\left(\rho C_p\right)_{nf}}{k_{nf}\left(\rho C_p\right)_f}, Q = \frac{Q_0 y'^2\left(\rho C_p\right)_f}{\left(\rho C_p\right)_{nf}}$$

$$M = \frac{\sigma B_0^2 \mu_{nf}\rho_f}{\mu_f \rho_{nf} v_r^{\,2}}, N = \frac{16\zeta T_0^3 \rho_f}{3\alpha\left(C_p\right)_{nf}}, Gr = \frac{g\beta_{nf}\left(T - T_0\right)\mu_{nf}}{v_0 u^2 \beta_f}, \chi = \frac{\upsilon\rho_f}{\rho_{nf}\kappa\mu_{nf}}$$

The plate in the x' – direction is considered infinite, therefore, all the physical variables are independent of the coordinate (Aruna et al [20]). Also, rewriting Eqs. (7) – (9) in dimensionless form, they are transformed into

$$\frac{\partial v}{\partial y} = 0 \tag{16}$$

$$\frac{\partial u}{\partial t} + v\frac{\partial u}{\partial y} = \frac{a_1}{\mathrm{Re}}\frac{\partial^2 u}{\partial y^2} - a_2\left(Ha + \chi\right)u + a_3 Gr\theta \tag{17}$$

$$\frac{\partial \theta}{\partial t} + v\frac{\partial \theta}{\partial y} = \frac{a_4}{\mathrm{Pr}}\frac{\partial^2 \theta}{\partial y^2} - a_5\left(N + Q\right)\theta \tag{18}$$

$$a_1 = \frac{1 + 2.5\phi + 6.2\phi^2}{1 - \phi + \phi\frac{\rho_s}{\rho_f}}, , \; a_2 = \left(1 - \phi + \phi\frac{\rho_s}{\rho_f}\right)^{-1} \; a_3 = 1 - \phi + \phi\frac{\beta_s}{\beta_f}$$

$$a_5 = \left(1-\phi+\phi\frac{(\rho C_p)_s}{(\rho C_p)_f}\right)^{-1} \quad a_4 = \left(1-\phi+\phi\frac{(\rho C_p)_s}{(\rho C_p)_f}\right)^{-1} \phi\frac{k_s}{k_f}+(1-\phi)$$

Subject to the transformed boundary conditions

$u=1,\ \theta=1+\varepsilon e^{nt},$ at $y=0$

$u\to 0,\ \theta\to 0,$ at $y\to\infty$ (19)

where Re is the Reynolds' number, Pr is the Prandtl number, Gr is the thermal Grashofs number, N is the dimensionless radiation term, θ is the dimensionless temperature, u is the dimensionless velocity, χ is the non-Darcy number, Ha is the magnetic Hartmann number and Q is the dimensionless heat function.

Method of solution

Solving, Eq.(16) is integrated and results in a constant or function of time and takes the form

$$v=-v_0\left(1+\varepsilon \mathrm{A}e^{i\omega t}\right) \quad (20)$$

Such that $\varepsilon \mathrm{A}<<1,\ \omega$ is free stream frequency and v_0 is a scale of suction velocity that has a non zero positive constant. The negative sign indicates that the suction velocity is towards the plate.

Following the transformation adopted by Mebine [21], a perturbation to transform the velocity and temperature models are given as

$$u(y,t)=u_0(y)e^{-\omega t} \quad (21)$$

$$\theta(y,t)=\theta_0(y)e^{-\omega t} \quad (22)$$

In view of Eqs. (20), (21) and (22), Eqs. (17) and (18) can be written as

$$u_0''(y)+\frac{\mathrm{Re}\left(1+\varepsilon \mathrm{A}e^{i\omega t}\right)u_0'(y)}{a_1}-\frac{\mathrm{Re}\left((Ha+\chi)a_2-\omega\right)u_0(y)}{a_1}+\frac{a_3\,\mathrm{Re}\,Gr\,\theta_0(y)}{a_1}=0 \quad (23)$$

$$\theta_0''(y)+\frac{\mathrm{Pr}\left(1+\varepsilon \mathrm{A}e^{i\omega t}\right)\theta_0'(y)}{a_4}-\frac{\mathrm{Pr}\left((N+Q)a_5-\omega\right)\theta_0(y)}{a_4}=0 \quad (24)$$

Applying the Homotopy Perturbation Method (HPM) to overcome the restriction of small perturbation parameters as used by He ([22], [23]) is to form the complex Homotopy as

$$H(\theta,p)=(1-p)\theta_0''(y)+p\left[\theta_0''(y)+\frac{\mathrm{Pr}\left(1+\varepsilon \mathrm{A}e^{i\omega t}\right)\theta_0'(y)}{a_4}-\frac{\mathrm{Pr}\left((N+Q)a_5-\omega\right)\theta_0(y)}{a_4}\right] \quad (25)$$

$$H(u,p)=(1-p)u_0''(y)+$$
$$p\left[u_0''(y)+\frac{\mathrm{Re}\left(1+\varepsilon \mathrm{A}e^{i\omega t}\right)u_0'(y)}{a_1}-\frac{\mathrm{Re}\left((Ha+\chi)a_2-\omega\right)u_0(y)}{a_1}+\frac{a_3\,\mathrm{Re}\,Gr\theta_0(y)}{a_1}\right] \quad (26)$$

Assume the solutions to Eqs. (25) and (26) be written as

$$\theta_0(y)=\theta_{00}(y)+p\theta_{01}(y)+p^2\theta_{02}(y)+..... \quad (27)$$

$$u_0(y)=u_{00}(y)+pu_{01}(y)+p^2u_{02}(y)+..... \quad (28)$$

Simplifying and comparing the coefficients p^0, p^1, p^2 and p^3 of Eqs. (25) and (26), the expressions are as follows

$$p^0:\ \theta_{00}''(y)=0 \quad (29)$$

$$p^0:\ u_{00}''(y)=0 \quad (30)$$

$$p^1:\ \theta_{01}''(y)+\frac{\mathrm{Pr}\left(1+\varepsilon \mathrm{A}e^{i\omega t}\right)\theta_{00}'(y)}{a_4}-\frac{\mathrm{Pr}\left((N+Q)a_5-\omega\right)\theta_{00}(y)}{a_4}=0 \quad (31)$$

$$p^1:\ u_{01}''(y)+\frac{\mathrm{Re}\left(1+\varepsilon \mathrm{A}e^{i\omega t}\right)u_{00}'(y)}{a_1}-\frac{\mathrm{Re}\left((Ha+\chi)-\omega\right)a_2u_{00}(y)}{a_1}+\frac{\mathrm{Re}\,a_3Gr\theta_{00}(y)}{a_1}=0 \quad (32)$$

$$p^2:\ \theta_{02}''(y)+\frac{\mathrm{Pr}\left(1+\varepsilon \mathrm{A}e^{i\omega t}\right)\theta_{01}'(y)}{a_4}-\frac{\mathrm{Pr}\left((N+Q)a_5-\omega\right)\theta_{01}(y)}{a_4}=0 \quad (33)$$

$$p^2:\ u_{02}''(y)+\frac{\mathrm{Re}\left(1+\varepsilon \mathrm{A}e^{i\omega t}\right)u_{01}'(y)}{a_1}-\frac{\mathrm{Re}\left((Ha+\chi)a_2-\omega\right)u_{01}(y)}{a_1}+\frac{\mathrm{Re}\,a_3Gr\theta_{01}(y)}{a_1}=0 \quad (34)$$

$$p^3:\ \theta_{03}''(y)+\frac{\mathrm{Pr}\left(1+\varepsilon \mathrm{A}e^{i\omega t}\right)\theta_{02}'(y)}{a_4}-\frac{\mathrm{Pr}\left((N+Q)a_5-\omega\right)\theta_{02}(y)}{a_4}=0 \quad (35)$$

$$p^3:\ u_{03}''(y)+\frac{\mathrm{Re}\left(1+\varepsilon \mathrm{A}e^{i\omega t}\right)u_{02}'(y)}{a_1}-\frac{\mathrm{Re}\left((Ha+\chi)a_2-\omega\right)u_{02}(y)}{a_1}+\frac{\mathrm{Re}\,a_3Gr\theta_{02}(y)}{a_1}=0 \quad (36)$$

$$\vdots$$

The transformed imposed boundary conditions are

$$u_{00}(0)=u_{01}(0)=u_{02}(0)=u_{03}(0)=...=e^{\omega t}$$

$$u_{00}(\infty)=u_{01}(\infty)=u_{02}(\infty)=u_{03}(\infty)=\ldots=0$$
$$\theta_{00}(0)=\theta_{01}(0)=\theta_{02}(0)=\theta_{03}(0)=\ldots=\left(1+\varepsilon e^{i\omega t}\right)e^{\omega t} \quad (37)$$
$$\theta_{00}(\infty)=\theta_{01}(\infty)=\theta_{02}(\infty)=\theta_{03}(\infty)=\ldots=0$$

Prime denotes derivative with respect to y.

The solutions to Eqs. (29) and (30) after imposing the appropriate boundary conditions of Eq. (37) are

$$\theta_{00}(y)=e^{\omega t}\left(1+\varepsilon e^{i\omega t}\right) \quad (38)$$

$$u_{00}(y)=e^{\omega t} \quad (39)$$

Similarly, the solutions to Eqs. (31) and (32) are respectively

$$\theta_{01}(y)=\frac{a_{12}}{2}e^{\omega t}\left(y^2-y\right)+\left(1+\varepsilon e^{i\omega t}\right)e^{\omega t} \quad (40)$$

$$u_{01}(y)=\frac{a_{14}}{2}e^{\omega t}\left(y^2-y\right)+\frac{a_{15}}{2}e^{\omega t}\left(1+\varepsilon e^{i\omega t}\right)\left(y-y^2\right)+e^{\omega t} \quad (41)$$

Also, the same method applied to Eqs. (33) and (34) respectively, results into

$$\theta_{02}(y)=-a_{11}\left(\frac{a_{12}}{2}e^{\omega t}\left(\frac{y^3}{3}-\frac{y^2}{2}\right)+\left(1+\varepsilon e^{i\omega t}\right)ye^{\omega t}\right)$$
$$-a_{12}\left(\frac{a_{12}}{2}e^{\omega t}\left(\frac{y^4}{12}-\frac{y^3}{6}\right)+\left(1+\varepsilon e^{i\omega t}\right)\frac{y^2}{2}e^{\omega t}\right)+a_{11}\left(\frac{a_{12}}{2}e^{\omega t}+\left(1+\varepsilon e^{\omega t}\right)e^{\omega t}\right)y \quad (42)$$
$$+a_{12}\left(\frac{a_{12}}{2}e^{\omega t}+\frac{1}{2}\left(1+\varepsilon e^{\omega t}\right)e^{\omega t}\right)y+e^{\omega t}\left(1+\varepsilon e^{i\omega t}\right)$$

$$u_{02}(y)=-a_{13}\left(\frac{a_{14}}{2}e^{\omega t}\left(\frac{y^3}{3}-\frac{y^2}{2}\right)+\frac{a_{15}}{2}e^{\omega t}\left(1+\varepsilon e^{i\omega t}\right)\left(\frac{y^2}{2}-\frac{y^3}{3}\right)+ye^{\omega t}\right)$$
$$+a_{14}a_2\left(\frac{a_{14}}{2}e^{\omega t}\left(\frac{y^4}{12}-\frac{y^3}{6}\right)+\frac{a_{15}}{2}e^{\omega t}\left(1+\varepsilon e^{i\omega t}\right)\left(\frac{y^3}{6}-\frac{y^4}{12}\right)+\frac{y^2}{2}e^{\omega t}\right) \quad (43)$$
$$-a_{15}\left(\frac{a_{12}}{2}e^{\omega t}\left(\frac{y^4}{12}-\frac{y^3}{6}\right)+\left(1+\varepsilon e^{i\omega t}\right)\frac{y^2}{2}e^{\omega t}\right)+$$
$$a_{13}\left(-\frac{a_{14}}{12}e^{\omega t}+\frac{a_{15}}{12}e^{\omega t}\left(1+\varepsilon e^{i\omega t}\right)+e^{\omega t}\right)y-a_{14}a_2\left(-\frac{a_{14}}{24}e^{\omega t}+\frac{a_{15}}{24}e^{\omega t}\left(1+\varepsilon e^{i\omega t}\right)+\frac{1}{2}e^{\omega t}\right)y$$
$$+a_{15}\left(\frac{a_{12}}{24}e^{\omega t}+\frac{1}{2}\left(1+\varepsilon e^{i\omega t}\right)e^{\omega t}\right)y+e^{\omega t}$$

Finally, following the same method and procedure, the solutions to Eqs. (35) and (36) result respectively into

$$\theta_{03}(y) =$$

$$-a_{11}\left[\begin{array}{l}(-\frac{a_{12}}{2}e^{\omega t}\left(\frac{y^4}{12}-\frac{y^3}{6}\right)+\left(1+\varepsilon e^{i\omega t}\right)\frac{y^2}{2}e^{\omega t})-a_{12}\left(\frac{a_{12}}{2}e^{\omega t}\left(\frac{y^5}{60}-\frac{y^4}{24}\right)+\left(1+\varepsilon e^{\omega t}\right)\frac{y^3}{6}e^{\omega t}\right)\\ +a_{11}\left(\frac{a_{12}}{2}e^{\omega t}+\left(1+\varepsilon e^{i\omega t}\right)e^{\omega t}\right)\frac{y^2}{2}+a_{12}\left(\frac{a_{12}}{2}e^{\omega t}+\frac{1}{2}\left(1+\varepsilon e^{\omega t}\right)e^{\omega t}\right)\frac{y^2}{2}+e^{\omega t}\left(1+\varepsilon e^{\omega t}\right)y\end{array}\right]$$

$$+a_{12}\left[\begin{array}{l}\left(-\frac{a_{12}}{2}e^{\omega t}\left(\frac{y^5}{60}-\frac{y^4}{24}\right)+\left(1+\varepsilon e^{\omega t}\right)\frac{y^3}{6}e^{\omega t}\right)-a_{12}\left(\frac{a_{12}}{2}e^{\omega t}\left(\frac{y^6}{360}-\frac{y^5}{120}\right)+\left(1+\varepsilon e^{\omega t}\right)\frac{y^4}{24}e^{\omega t}\right)\\ +a_{11}\left(\frac{a_{12}}{2}e^{\omega t}+\left(1+\varepsilon e^{\omega t}\right)e^{\omega t}\right)\frac{y^3}{6}+a_{12}\left(\frac{a_{12}}{2}e^{\omega t}+\left(\frac{1+\varepsilon e^{i\omega t}}{2}\right)e^{\omega t}\right)\frac{y^3}{6}+e^{\omega t}\left(1+\varepsilon e^{\omega t}\right)\frac{y^2}{2}\end{array}\right]$$

$$+a_{11}\left[\begin{array}{l}(\frac{a_{12}}{24}e^{\omega t}+\left(1+\varepsilon e^{i\omega t}\right)\frac{1}{2}e^{\omega t})-a_{12}\left(-\frac{a_{12}}{40}e^{\omega t}+\left(1+\varepsilon e^{\omega t}\right)\frac{1}{6}e^{\omega t}\right)\\ +a_{11}\left(\frac{a_{12}}{2}e^{\omega t}+\left(1+\varepsilon e^{i\omega t}\right)e^{\omega t}\right)\frac{1}{2}+a_{12}\left(\frac{a_{12}}{2}e^{\omega t}+\frac{1}{2}\left(1+\varepsilon e^{\omega t}\right)e^{\omega t}\right)\frac{1}{2}+e^{\omega t}\left(1+\varepsilon e^{\omega t}\right)\end{array}\right]y$$

$$-a_{12}\left[\begin{array}{l}\left(\frac{a_{12}}{40}e^{\omega t}+\left(1+\varepsilon e^{\omega t}\right)\frac{1}{6}e^{\omega t}\right)-a_{12}\left(-\frac{a_{12}}{180}e^{\omega t}+\left(1+\varepsilon e^{\omega t}\right)\frac{1}{24}e^{\omega t}\right)\\ +a_{11}\left(\frac{a_{12}}{2}e^{\omega t}+\left(1+\varepsilon e^{\omega t}\right)e^{\omega t}\right)\frac{1}{6}+a_{12}\left(\frac{a_{12}}{2}e^{\omega t}+\left(\frac{1+\varepsilon e^{i\omega t}}{2}\right)e^{\omega t}\right)\frac{1}{6}+\\ e^{\omega t}\left(1+\varepsilon e^{\omega t}\right)\frac{1}{2}\end{array}\right]y \qquad (44)$$

$$+\left(1+\varepsilon e^{i\omega t}\right)$$

$$u_{03}(y) = a^2{}_{13}\left(\frac{a_{14}}{2}e^{\omega t}\left(\frac{y^5}{60}-\frac{y^4}{24}\right)-\frac{a_{13}a_{15}}{2}e^{\omega t}\left(1+\varepsilon e^{i\omega t}\right)\left(\frac{y^4}{24}-\frac{y^5}{60}\right)-\frac{y^3}{6}e^{\omega t}\right)$$

$$-a_{13}a_{14}a_2\left(\frac{a_{14}}{2}e^{\omega t}\left(\frac{y^6}{360}-\frac{y^5}{120}\right)-\frac{a_{13}a_{15}}{2}e^{\omega t}\left(1+\varepsilon e^{i\omega t}\right)\left(\frac{y^5}{120}-\frac{y^6}{360}\right)-\frac{y^4}{24}e^{\omega t}\right) \qquad (45)$$

$$+a_{13}a_{15}\left(\frac{a_{12}}{2}e^{\omega t}\left(\frac{y^6}{360}-\frac{y^5}{120}\right)-\left(1+\varepsilon e^{i\omega t}\right)\frac{y^4}{24}e^{\omega t}\right)-$$

$$a^2{}_{13}\left(-\frac{a_{14}}{12}e^{\omega t}+\frac{a_{15}}{12}e^{\omega t}\left(1+\varepsilon e^{i\omega t}\right)+e^{\omega t}\right)\frac{y^3}{6}+a_{13}a_{14}a_2\left(-\frac{a_{14}}{24}e^{\omega t}+\frac{a_{15}}{24}e^{\omega t}\left(1+\varepsilon e^{i\omega t}\right)+\frac{1}{2}e^{\omega t}\right)\frac{y^3}{6}$$

$$-a_{13}a_{15}\left(\frac{a_{12}}{24}e^{\omega t}+\frac{1}{2}\left(1+\varepsilon e^{i\omega t}\right)e^{\omega t}\right)\frac{y^3}{6}-\frac{y^2}{2}e^{\omega t}+$$

$$a_2a_{14}a_{13}\left(\frac{a_{14}}{2}e^{\omega t}\left(\frac{y^4}{12}-\frac{y^3}{6}\right)+\frac{a_2a_{14}a_{15}}{2}e^{\omega t}\left(1+\varepsilon e^{i\omega t}\right)\left(\frac{y^3}{6}-\frac{y^4}{12}\right)+\frac{y^2}{2}e^{\omega t}\right)$$

$$-a^2{}_{14}a^2{}_2\left(\frac{a_{14}}{2}e^{\omega t}\left(\frac{y^5}{60}-\frac{y^4}{24}\right)-\frac{a_2a_{14}a_{15}}{2}e^{\omega t}\left(1+\varepsilon e^{i\omega t}\right)\left(\frac{y^4}{24}-\frac{y^5}{60}\right)+\frac{y^3}{6}e^{\omega t}\right)$$

$$-a_2a_{14}a_{15}\left(\frac{a_{12}}{2}e^{\omega t}\left(\frac{y^5}{60}-\frac{y^4}{24}\right)-a_2a_{14}\left(1+\varepsilon e^{i\omega t}\right)\frac{y^3}{6}e^{\omega t}\right)+$$

$$a_2a_{14}a_{13}\left(-\frac{a_{14}}{12}e^{\omega t}+\frac{a_{15}}{12}e^{\omega t}\left(1+\varepsilon e^{i\omega t}\right)+e^{\omega t}\right)\frac{y^2}{2}+a^2{}_{14}a^2{}_2\left(-\frac{a_{14}}{24}e^{\omega t}+\frac{a_{15}}{24}e^{\omega t}\left(1+\varepsilon e^{i\omega t}\right)+\frac{1}{2}e^{\omega t}\right)\frac{y^2}{2}$$

$$-a_2a_{14}a_{15}\left(\frac{a_{12}}{24}e^{\omega t}+\frac{1}{2}\left(1+\varepsilon e^{i\omega t}\right)e^{\omega t}\right)\frac{y^2}{2}-a_2a_{14}ye^{\omega t}$$

$$+a^2{}_{13}\left(\frac{a_{14}}{80}e^{\omega t}+\frac{a_{13}a_{15}}{80}e^{\omega t}\left(1+\varepsilon e^{i\omega t}\right)+\frac{1}{6}e^{\omega t}\right)y-$$

$$a_{13}a_{14}a_2\left(\frac{a_{14}}{360}e^{\omega t}+\frac{a_{13}a_{15}}{360}e^{\omega t}\left(1+\varepsilon e^{i\omega t}\right)+\frac{1}{24}e^{\omega t}\right)y+a_{13}a_{15}\left(\frac{a_{12}}{360}e^{\omega t}+\left(1+\varepsilon e^{i\omega t}\right)\frac{1}{24}e^{\omega t}\right)y+$$

$$a^2{}_{13}\left(-\frac{a_{14}}{12}e^{\omega t}+\frac{a_{15}}{12}e^{\omega t}\left(1+\varepsilon e^{i\omega t}\right)+e^{\omega t}\right)\frac{y}{6}-a_{13}a_{14}a_2\left(-\frac{a_{14}}{24}e^{\omega t}+\frac{a_{15}}{24}e^{\omega t}\left(1+\varepsilon e^{i\omega t}\right)+\frac{1}{2}e^{\omega t}\right)\frac{y}{6}$$

$$+a_{13}a_{15}\left(\frac{a_{12}}{24}e^{\omega t}+\frac{1}{2}\left(1+\varepsilon e^{i\omega t}\right)e^{\omega t}\right)\frac{y}{6}+\frac{y}{2}e^{\omega t}$$

$$-a_2a_{14}a_{13}\left(\frac{a_{14}}{24}e^{\omega t}-\frac{a_2a_{14}a_{15}}{24}e^{\omega t}\left(1+\varepsilon e^{i\omega t}\right)-\frac{1}{2}e^{\omega t}\right)y$$

$$+a^2{}_{14}a^2{}_2\left(-\frac{a_{14}}{80}e^{\omega t}-\frac{a_2a_{14}a_{15}}{80}e^{\omega t}\left(1+\varepsilon e^{i\omega t}\right)+\frac{1}{6}e^{\omega t}\right)y+a_2a_{14}a_{15}\left(-\frac{a_{12}}{80}e^{\omega t}-a_2a_{14}\left(1+\varepsilon e^{i\omega t}\right)\frac{1}{6}e^{\omega t}\right)y+$$

$$a_2a_{14}a_{13}\left(-\frac{a_{14}}{12}e^{\omega t}+\frac{a_{15}}{12}e^{\omega t}\left(1+\varepsilon e^{i\omega t}\right)+e^{\omega t}\right)\frac{y}{2}+$$

$$a^2{}_{14}a^2{}_2\left(-\frac{a_{14}}{24}e^{\omega t}+\frac{a_{15}}{24}e^{\omega t}\left(1+\varepsilon e^{i\omega t}\right)+\frac{1}{2}e^{\omega t}\right)\frac{y}{2}-a_2a_{14}a_{15}\left(\frac{a_{12}}{24}e^{\omega t}+\frac{1}{2}\left(1+\varepsilon e^{i\omega t}\right)e^{\omega t}\right)\frac{y}{2}-a_2a_{14}ye^{\omega t}$$

$$+a_{11}a_{15}\left(-\frac{a_{12}}{24}e^{\omega t}-\left(1+\varepsilon e^{i\omega t}\right)\frac{1}{2}e^{\omega t}\right)y$$

$$+a_{15}a_{12}\left(-\frac{a_{12}}{40}e^{\omega t}+\left(1+\varepsilon e^{i\omega t}\right)\frac{1}{6}e^{\omega t}\right)y-a_{15}a_{11}\left(\frac{a_{12}}{2}e^{\omega t}+\left(1+\varepsilon e^{\omega t}\right)e^{\omega t}\right)\frac{y}{2}$$

$$-a_{15}a_{12}\left(\frac{a_{12}}{2}e^{\omega t}+\frac{1}{2}\left(1+\varepsilon e^{\omega t}\right)e^{\omega t}\right)\frac{y}{2}-a_{15}e^{\omega t}\left(1+\varepsilon e^{i\omega t}\right)y+e^{\omega t}$$

where

$$a_{11}=\frac{\Pr\left(1+\varepsilon e^{i\omega t}\right)}{a_4},\ a_{12}=\frac{\Pr\left((N+Q)-\omega\right)}{a_4},\ a_{13}=\frac{\mathrm{Re}\left(1+\varepsilon e^{i\omega t}\right)}{a_1},\ a_{14}=\frac{\mathrm{Re}\left((Ha+\chi)a_2-\omega\right)}{a_1}$$

$$a_{15}=\frac{\mathrm{Re}\,a_3 Gr}{a_1}$$

The solution of the velocity and temperature fields are respectively given as

$$u_0(y)=u_{00}(y)+u_{01}(y)+u_{02}(y)+u_{03}(y)+\ldots\ldots\ldots \quad (46)$$

$$\theta_0(y)=\theta_{00}(y)+\theta_{01}(y)+\theta_{02}(y)+\theta_{03}(y)+\ldots\ldots\ldots \quad (47)$$

The complete solution is obtained by putting Eq. (46) into Eq. (21) and Eq. (47) into Eq. (22), the results are respectively;

$$u(y,t)e^{\omega t}=u_{00}(y)+u_{01}(y)+u_{02}(y)+u_{03}(y)+\ldots\ldots\ldots \quad (48)$$

$$\theta(y,t)e^{\omega t}=\theta_{00}(y)+\theta_{01}(y)+\theta_{02}(y)+\theta_{03}(y)+\ldots\ldots\ldots \quad (49)$$

However, most models for physical description are governed by second order differential equations (ordinary and partial differential equations), therefore, Eqs. (48) and (49), reduced to take the form

$$u(y,t)=4+\frac{a_{14}}{2}\left(y^2-y\right)+\frac{a_{15}}{2}\left(1+\varepsilon e^{i\omega t}\right)\left(y-y^2\right)$$
$$-a_{13}\left(-\frac{y^2}{2}+\frac{a_{14}}{2}\left(-\frac{y^2}{2}\right)+\frac{a_{15}}{2}\left(1+\varepsilon e^{i\omega t}\right)\left(\frac{y^2}{2}\right)+y\right)+a_{14}a_2\left(\frac{y^2}{2}\right)-a_{15}\left(\left(1+\varepsilon e^{i\omega t}\right)\frac{y^2}{2}\right)+$$
$$a_{13}\left(-\frac{a_{14}}{12}+\frac{a_{15}}{12}\left(1+\varepsilon e^{i\omega t}\right)+1\right)y-a_{14}a_2\left(-\frac{a_{14}}{24}+\frac{a_{15}}{24}\left(1+\varepsilon e^{i\omega t}\right)+\frac{1}{2}\right)y$$
$$+a_{15}\left(\frac{a_{12}}{24}+\frac{1}{2}\left(1+\varepsilon e^{i\omega t}\right)\right)y+a_2a_{14}a_{13}\left(\frac{a_2a_{14}a_{15}}{4}\left(1+\varepsilon e^{i\omega t}\right)y^2\right)$$
$$+a_2a_{14}a_{13}\left(-\frac{a_{14}}{12}+\frac{a_{15}}{12}\left(1+\varepsilon e^{i\omega t}\right)+\right)\frac{y^2}{2}+a^2{}_{14}a^2{}_2\left(-\frac{a_{14}}{24}+\frac{a_{15}}{24}\left(1+\varepsilon e^{i\omega t}\right)+\frac{1}{2}\right)\frac{y^2}{2}$$
$$-a_2a_{14}a_{15}\left(\frac{a_{12}}{24}+\frac{1}{2}\left(1+\varepsilon e^{i\omega t}\right)\right)\frac{y^2}{2}-a_2a_{14}y+$$
$$a^2{}_{13}\left(\frac{a_{14}}{80}+\frac{a_{13}a_{15}}{80}\left(1+\varepsilon e^{i\omega t}\right)+\frac{1}{6}\right)y-a_{13}a_{14}a_2\left(\frac{a_{14}}{360}+\frac{a_{13}a_{15}}{360}\left(1+\varepsilon e^{i\omega t}\right)+\frac{1}{24}\right)y$$
$$+a_{13}a_{15}\left(\frac{a_{12}}{360}+\left(1+\varepsilon e^{i\omega t}\right)\frac{1}{24}\right)y+$$

$$a^2{}_{13}\left(-\frac{a_{14}}{12}+\frac{a_{15}}{12}\left(1+\varepsilon e^{i\omega t}\right)\right)\frac{y}{6}-a_{13}a_{14}a_2\left(-\frac{a_{14}}{24}+\frac{a_{15}}{24}\left(1+\varepsilon e^{i\omega t}\right)+\frac{1}{2}\right)\frac{y}{6}$$
$$+a_{13}a_{15}\left(\frac{a_{12}}{24}+\frac{1}{2}\left(1+\varepsilon e^{i\omega t}\right)\right)\frac{y}{6}+\frac{y}{2}$$
$$-a_2a_{14}a_{13}\left(\frac{a_{14}}{24}-\frac{a_2a_{14}a_{15}}{24}\left(1+\varepsilon e^{i\omega t}\right)-\frac{1}{2}\right)y+a^2{}_{14}a^2{}_2\left(-\frac{a_{14}}{80}-\frac{a_2a_{14}a_{15}}{80}\left(1+\varepsilon e^{i\omega t}\right)+\frac{1}{6}\right)y$$
$$+a_2a_{14}a_{15}\left(-\frac{a_{12}}{80}-a_2a_{14}\left(1+\varepsilon e^{i\omega t}\right)\frac{1}{6}\right)y+$$
$$a_2a_{14}a_{13}\left(-\frac{a_{14}}{12}+\frac{a_{15}}{12}\left(1+\varepsilon e^{i\omega t}\right)+1\right)\frac{y}{2}+a^2{}_{14}a^2{}_2\left(-\frac{a_{14}}{24}+\frac{a_{15}}{24}\left(1+\varepsilon e^{i\omega t}\right)+\frac{1}{2}\right)\frac{y}{2} \quad (50)$$
$$-a_2a_{14}a_{15}\left(\frac{a_{12}}{24}+\frac{1}{2}\left(1+\varepsilon e^{i\omega t}\right)\right)\frac{y}{2}-a_2a_{14}y+$$
$$a_{11}a_{15}\left(-\frac{a_{12}}{24}-\left(1+\varepsilon e^{i\omega t}\right)\frac{1}{2}\right)y+a_{15}a_{12}\left(-\frac{a_{12}}{40}+\left(1+\varepsilon e^{i\omega t}\right)\frac{1}{6}\right)y-a_{15}a_{11}\left(\frac{a_{12}}{2}+\left(1+\varepsilon e^{\omega t}\right)\right)\frac{y}{2}$$
$$-a_{15}a_{12}\left(\frac{a_{12}}{2}+\frac{1}{2}\left(1+\varepsilon e^{\omega t}\right)\right)\frac{y}{2}-a_{15}\left(1+\varepsilon e^{i\omega t}\right)y+\ldots$$

$$\theta(y,t)=4\left(1+\varepsilon e^{i\omega t}\right)+\frac{a_{12}}{2}\left(y^2-y\right)+$$
$$-a_{11}\left(\frac{a_{12}}{2}\left(-\frac{y^2}{2}\right)+\left(1+\varepsilon e^{i\omega t}\right)y\right)+a_{11}\left(\frac{a_{12}}{2}+\left(1+\varepsilon e^{\omega t}\right)\right)y+a_{12}\left(\frac{a_{12}}{2}+\frac{1}{2}\left(1+\varepsilon e^{\omega t}\right)\right)y$$

$$-a_{11}\left[\left(1+\varepsilon e^{i\omega t}\right)\frac{y^2}{2}+a_{11}\left(\frac{a_{12}}{2}+\left(1+\varepsilon e^{i\omega t}\right)\right)\frac{y^2}{2}+a_{12}\left(\frac{a_{12}}{2}+\frac{1}{2}\left(1+\varepsilon e^{\omega t}\right)\right)\frac{y^2}{2}+\left(1+\varepsilon e^{\omega t}\right)y\right]$$

$$+a_{11}\left[\begin{array}{l}\left(\frac{a_{12}}{24}+\left(1+\varepsilon e^{i\omega t}\right)\frac{1}{2}\right)-a_{12}\left(-\frac{a_{12}}{40}+\left(1+\varepsilon e^{\omega t}\right)\frac{1}{6}\right)+\\ a_{11}\left(\frac{a_{12}}{2}+\left(1+\varepsilon e^{i\omega t}\right)\right)\frac{1}{2}+a_{12}\left(\frac{a_{12}}{2}+\frac{1}{2}\left(1+\varepsilon e^{\omega t}\right)\right)\frac{1}{2}+\left(1+\varepsilon e^{\omega t}\right)\end{array}\right]y \quad (51)$$
$$-a_{12}\left[\begin{array}{l}\left(\frac{a_{12}}{40}+\left(1+\varepsilon e^{\omega t}\right)\frac{1}{6}\right)-a_{12}\left(-\frac{a_{12}}{180}+\left(1+\varepsilon e^{\omega t}\right)\frac{1}{24}\right)\\ +a_{11}\left(\frac{a_{12}}{2}+\left(1+\varepsilon e^{\omega t}\right)\right)\frac{1}{6}+a_{12}\left(\frac{a_{12}}{2}+\left(\frac{1+\varepsilon e^{i\omega t}}{2}\right)\right)\frac{1}{6}+\left(1+\varepsilon e^{\omega t}\right)\frac{1}{2}\end{array}\right]y$$

Skin friction (τ) and Mass transfer coefficient (Nu)

The skin friction is determined by the relation

$\tau = \left.\frac{\partial u}{\partial y}\right|_{y=0}$ and Eq. (50) is reduced to the form

$$\tau = -\frac{a_{14}}{2} + \frac{a_{15}}{2}\left(1+\varepsilon e^{i\omega t}\right) + a_{13}\left(-\frac{a_{14}}{12} + \frac{a_{15}}{12}\left(1+\varepsilon e^{i\omega t}\right)\right)$$
$$- a_{14}a_2\left(-\frac{a_{14}}{24} + \frac{a_{15}}{24}\left(1+\varepsilon e^{i\omega t}\right) + \frac{1}{2}\right) + a_{15}\left(\frac{a_{12}}{24} + \frac{1}{2}\left(1+\varepsilon e^{i\omega t}\right)\right) - 2a_2a_{14}$$
$$+ a^2{}_{13}\left(\frac{a_{14}}{80} + \frac{a_{13}a_{15}}{80}\left(1+\varepsilon e^{i\omega t}\right) + \frac{1}{6}\right) - a_{13}a_{14}a_2\left(\frac{a_{14}}{360} + \frac{a_{13}a_{15}}{360}\left(1+\varepsilon e^{i\omega t}\right) + \frac{1}{24}\right)$$
$$+ a_{13}a_{15}\left(\frac{a_{12}}{360} + \left(1+\varepsilon e^{i\omega t}\right)\frac{1}{24}\right) +$$
$$a^2{}_{13}\left(-\frac{a_{14}}{72} + \frac{a_{15}}{72}\left(1+\varepsilon e^{i\omega t}\right)\right) - a_{13}a_{14}a_2\left(-\frac{a_{14}}{144} + \frac{a_{15}}{144}\left(1+\varepsilon e^{i\omega t}\right) + \frac{1}{12}\right)$$
$$+ a_{13}a_{15}\left(\frac{a_{12}}{144} + \frac{1}{12}\left(1+\varepsilon e^{i\omega t}\right)\right) + \frac{1}{2}$$
$$- a_2a_{14}a_{13}\left(\frac{a_{14}}{24} - \frac{a_2a_{14}a_{15}}{24}\left(1+\varepsilon e^{i\omega t}\right) - \frac{1}{2}\right) + a^2{}_{14}a^2{}_2\left(-\frac{a_{14}}{80} - \frac{a_2a_{14}a_{15}}{80}\left(1+\varepsilon e^{i\omega t}\right) + \frac{1}{6}\right)$$
$$+ a_2a_{14}a_{15}\left(-\frac{a_{12}}{480} - \frac{a_2a_{14}}{6}\left(1+\varepsilon e^{i\omega t}\right)\right) +$$
$$a_2a_{14}a_{13}\left(-\frac{a_{14}}{24} + \frac{a_{15}}{24}\left(1+\varepsilon e^{i\omega t}\right) + \frac{1}{2}\right) + a^2{}_{14}a^2{}_2\left(-\frac{a_{14}}{48} + \frac{a_{15}}{48}\left(1+\varepsilon e^{i\omega t}\right) + \frac{1}{4}\right) \quad (52)$$
$$- a_2a_{14}a_{15}\left(\frac{a_{12}}{48} + \frac{1}{4}\left(1+\varepsilon e^{i\omega t}\right)\right) +$$
$$a_{11}a_{15}\left(-\frac{a_{12}}{24} - \frac{1}{2}\left(1+\varepsilon e^{i\omega t}\right)\right) + a_{15}a_{12}\left(-\frac{a_{12}}{40} + \frac{1}{6}\left(1+\varepsilon e^{i\omega t}\right)\right) - a_{15}a_{11}\left(\frac{a_{12}}{4} + \frac{1}{2}\left(1+\varepsilon e^{\omega t}\right)\right)$$
$$- a_{15}a_{12}\left(\frac{a_{12}}{4} + \frac{1}{4}\left(1+\varepsilon e^{\omega t}\right)\right) - a_{15}\left(1+\varepsilon e^{i\omega t}\right) + \ldots$$

In the same vein, the heat transfer coefficient which is the Nusselt number is given as $Nu = -\left.\frac{\partial \theta}{\partial y}\right|_{y=0}$ and the result is

$$Nu = \frac{a_{12}}{2} + 2a_{11}\left(\left(1+\varepsilon e^{i\omega t}\right)\right) - a_{11}\left(\frac{a_{12}}{2} + \left(1+\varepsilon e^{\omega t}\right)\right) - a_{12}\left(\frac{a_{12}}{2} + \frac{1}{2}\left(1+\varepsilon e^{\omega t}\right)\right)$$

$$-a_{11}\left[\begin{array}{l}\frac{a_{12}}{24}+\frac{1}{2}\left(1+\varepsilon e^{i\omega t}\right)-a_{12}\left(-\frac{a_{12}}{40}+\frac{1}{6}\left(1+\varepsilon e^{i\omega t}\right)\right)+\\ a_{11}\left(\frac{a_{12}}{4}+\frac{1}{2}\left(1+\varepsilon e^{i\omega t}\right)\right)+a_{12}\left(\frac{a_{12}}{4}+\frac{1}{4}\left(1+\varepsilon e^{i\omega t}\right)\right)+\left(1+\varepsilon e^{i\omega t}\right)\end{array}\right]$$
$$+a_{12}\left[\begin{array}{l}\left(\frac{a_{12}}{40}+\frac{1}{6}\left(1+\varepsilon e^{i\omega t}\right)\right)-a_{12}\left(-\frac{a_{12}}{180}+\frac{1}{24}\left(1+\varepsilon e^{i\omega t}\right)\right)\\ +a_{11}\left(\frac{a_{12}}{12}+\frac{1}{6}\left(1+\varepsilon e^{i\omega t}\right)\right)+a_{12}\left(\frac{a_{12}}{12}+\left(\frac{1+\varepsilon e^{i\omega t}}{12}\right)\right)+\frac{1}{2}\left(1+\varepsilon e^{i\omega t}\right)\end{array}\right] \quad (53)$$

Results and Discussion

Results

Table 2: Showing different values of Nusselt number (Nu) and skin friction (τ) for varying some material parameters. $\varepsilon A = 0.01, \omega = 2.3$

Pr	Re	Gr	N	Q >0	Q <0	Ha	χ	$\phi\ x10^{-9}$	Nu	τ
0.7	100	1.3	1.97	3.51	0.00	0.15	0.1	3.0	-0.595189	$4.52832x10^{7}$
3.0									377.314	$4.52831x10^{7}$
5.0									2780.99	$4.52800x10^{7}$
7.0									10200	$4.52718x10^{7}$
	1000								-0.595189	$4.61848x10^{11}$
	3000								-0.595189	$3.74656x10^{13}$
	4000								-0.595189	$1.18432x10^{14}$
		2.3							0.595189	$8.01582x10^{7}$
		3.3							0.595189	$1.15033x10^{8}$
		4.3							0.595189	$1.49908x10^{8}$
			5.97						7.55725	$1.49912x10^{8}$
			11.97						62.6214	$1.49915x10^{8}$
			15.97						144.889	$1.49917x10^{8}$
				7.51					7.55725	$1.49912x10^{8}$
				10.51					26.7514	$1.49914x10^{8}$
				13.51					62.6214	$1.49915x10^{8}$
					-3.51				0.353739	$8.41244x10^{6}$
					-7.51				-10.5126	$8.41052x10^{6}$
					-10.51				-33.6351	$8.40869x10^{6}$
					-13.51				-73.3417	$8.40652x10^{6}$
							0.95		62.6214	$5.39992x10^{7}$

		1.75	**62.6214**	$1.33645x10^7$
		3.75	**62.6214**	$3.37939x10^7$
	0.6		**62.6214**	$8.25085x10^7$
	0.9		**62.6214**	$5.39992x10^7$
	1.3		**62.6214**	$2.7913x10^7$
5.0			**-0.566739**	$8.441435x10^7$
7.0			**-0.529812**	$8.441435x10^7$
9.0			**-0.483881**	$8.441435x10^7$

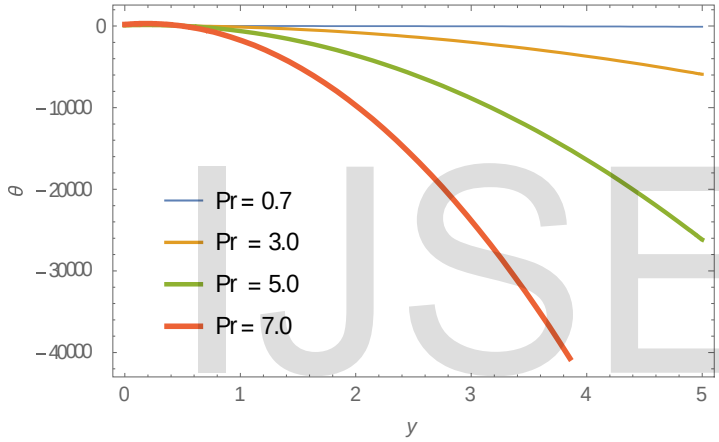

Fig.2: The dependence of temperature on coordinate with Prandtl number (Pr) varying

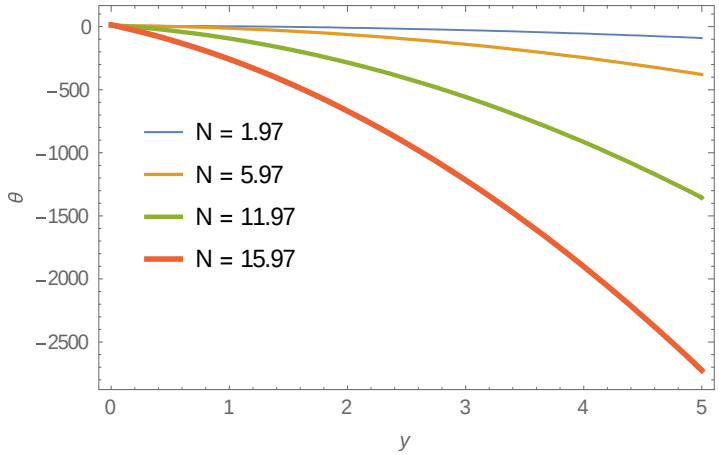

Fig.3: The dependence of temperature on coordinate with Radiation term (N) varying

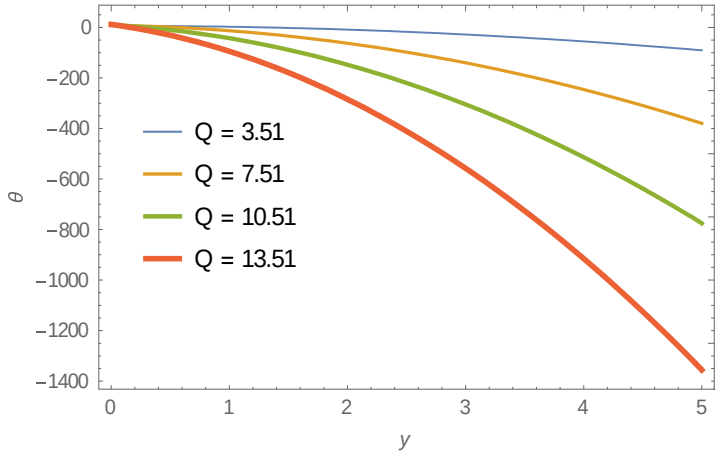

Fig.4: The dependence of temperature on coordinate with Heat source term (Q > 0) varying

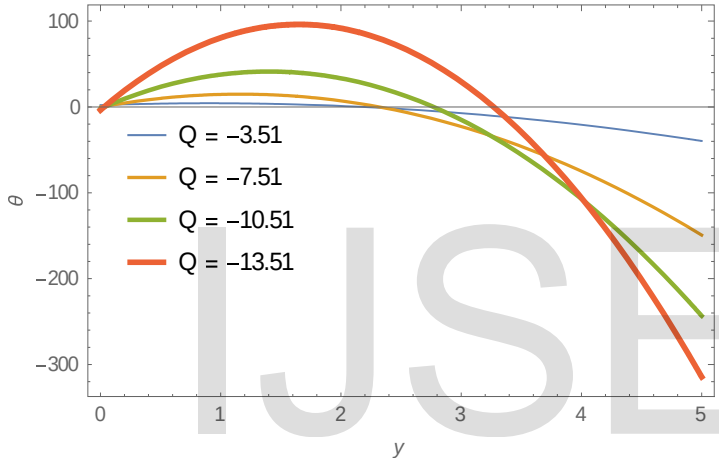

Fig.5: The dependence of temperature on coordinate with heat sink term (Q < 0) varying

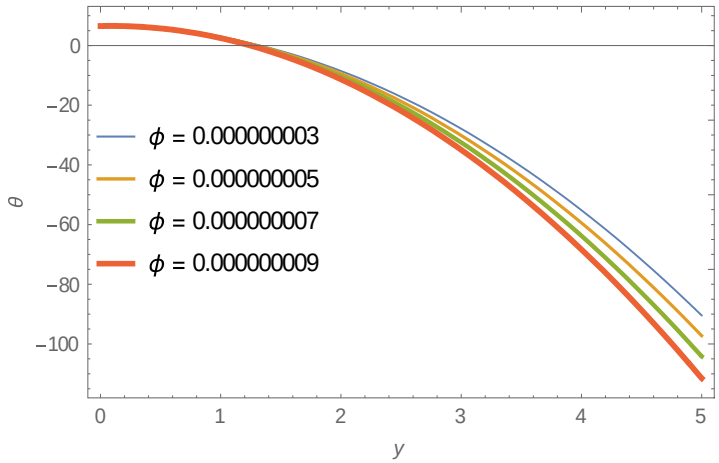

Fig.6: The dependence of temperature on coordinate with Nanoparticle volume fractions (ϕ) varying

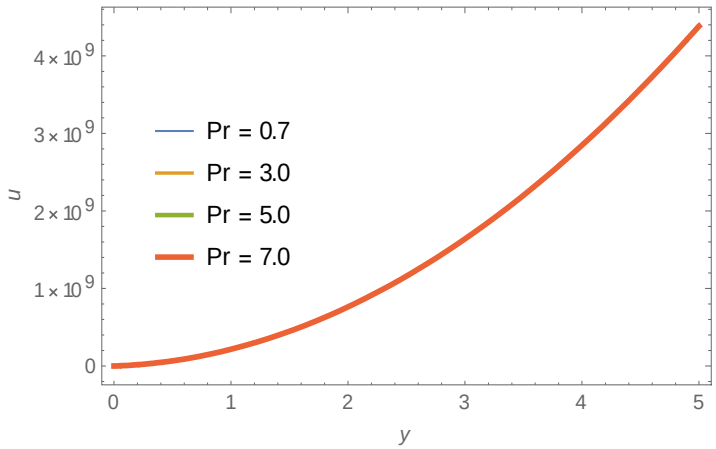

Fig.7: The dependence of velocity on coordinate with Prandtl number (Pr) varying

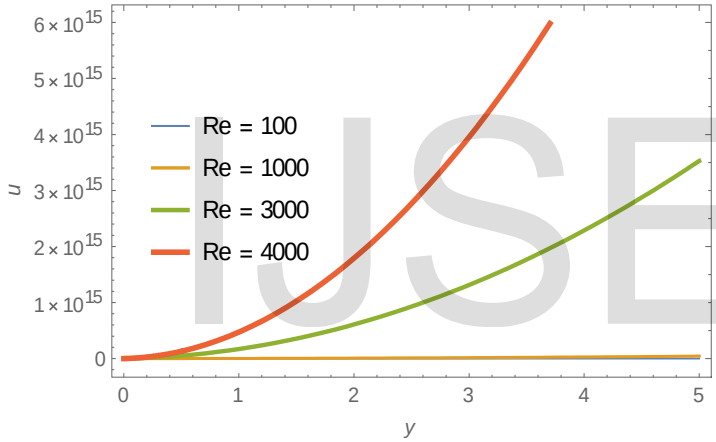

Fig.8: The dependence of velocity on coordinate with Reynolds number (Re) varying

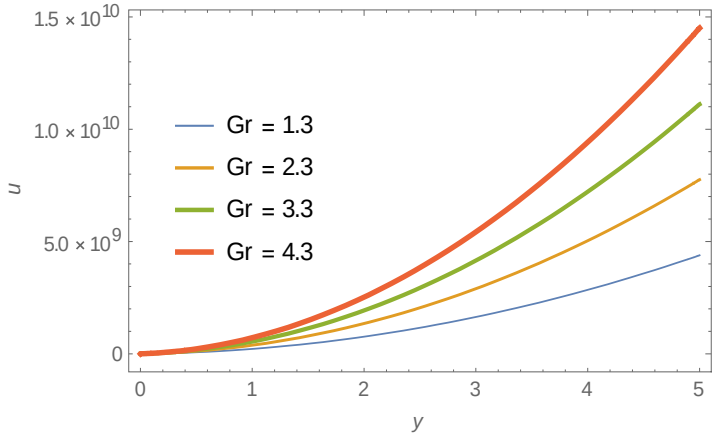

Fig.9: The dependence of velocity on coordinate with Grashof number (Gr) varying

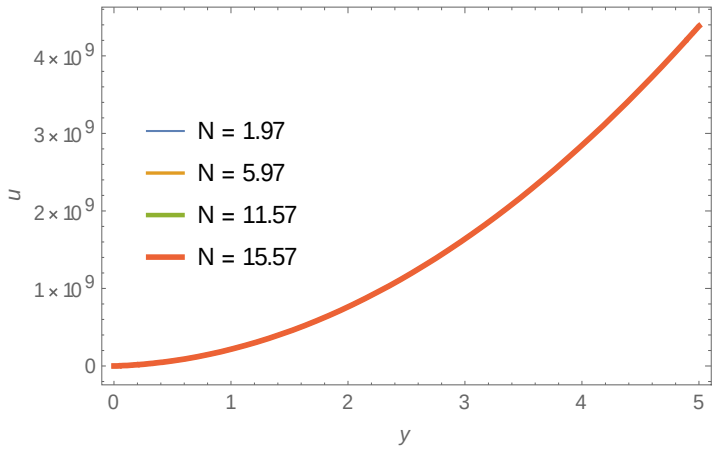

Fig.10: The dependence of velocity on coordinate with Radiation term (N) varying

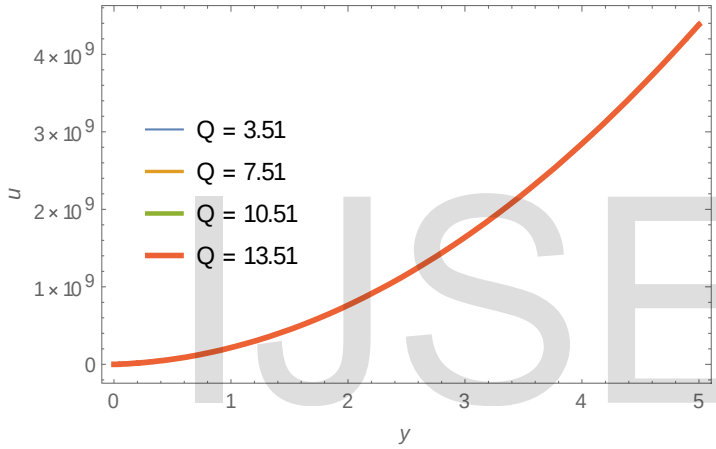

Fig.11: The dependence of velocity on coordinate with heat source term (Q > 0) varying

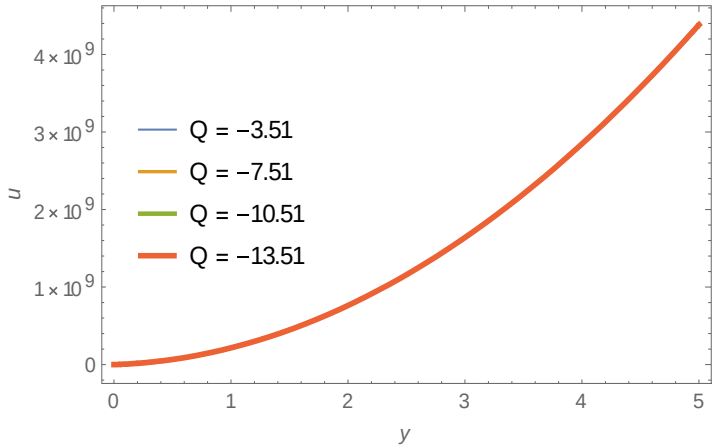

Fig.12: The dependence of velocity on coordinate with heat sink term (Q < 0) varying

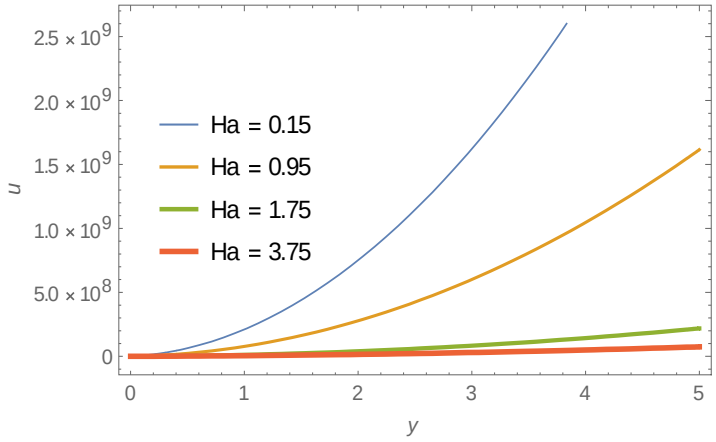

Fig.13: The dependence of velocity on coordinate with Hartmann number (Ha) varying

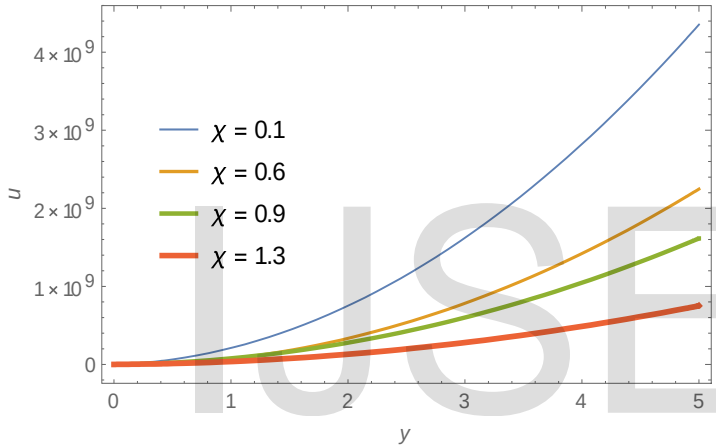

Fig.14: The dependence of velocity on coordinate with non-Darcian term (χ) varying

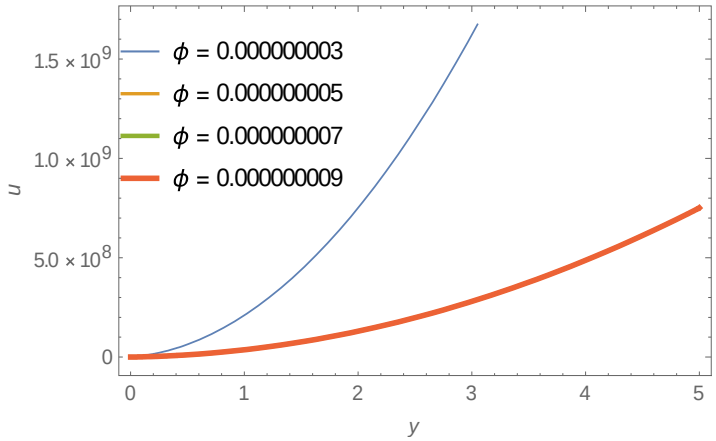

Fig.15: The dependence of velocity on coordinate with nanoparticle volume fractions (ϕ) varying

Discussion

The problem of the thermal effects on MHD convective flow of alumina nanofluid through a non-Darcian porous plate using HPM is analyzed. Following the solution

of the governing hydrodynamic equations, numerical computations was done for the Nusselt number and skin friction while graphical illustrations for temperature fields as well as the velocity fields for various values of the nanofluid material parameters were carried out. Table 2, showed that an increase in Pr, Ha, and χ diminished the skin friction of the nanofluid at the wall of the plate while the N, Q, Gr and Re enhanced the skin friction. However, the skin friction is unaffected by ϕ. The observations are consistent with the works of Wang and Mujumdar [6] and Karthikeyan et al [13] and when compared with the works of Polidori et al [10] and Mansour et al [11], they all followed the same trend. Similarly, increase in Pr, N, Q > 0 and ϕ correspond to an increase in the heat transfer coefficient and in agreement with the works of Karthikeyan et al [13], Polidori et al [10] and Mansour et al [11] but the Nusselt number is unaffected by increase in Re, Gr, Ha, and χ. A decrease is observed in Nusselt number as Q < 0 increases. The Prandtl number sheds light on the relative importance of viscous dissipation to the thermal dissipation. An increase in the Prandtl number from air (Pr = 0.7) to water (Pr = 7.0), decreases not only the thermal boundary thickness but also the mean temperature within the boundary layer. It is therefore shown from Fig.2 and Fig.7 that an increase in the Prandtl number, results in a corresponding decrease in the temperature profile and velocity profile of the alumina nanofluid. This observation is consistent with the findings of Karthikeyan et al [13], Makinde and Mukutu [24] and Ngiangia and Akazue [25] and followed the same trend when compared with the studies of Polidori et al [10] and Mansour et al [11]. An increase in the radiation term (N) as depicted in Fig.3 and Fig.10, revealed that the temperature and velocity profiles of the nanofluid are increased. The results are in agreement with the works of Karthikeyan et al [13], Aaiza et al [18] and Ngiangia and Akazue [25]. An analysis of Fig.4 and Fig.11 showed an increase in the Q > 0 and the result led to a decrease in both the temperature and velocity profiles of the nanofluid. The observations are the same with the findings of Karthikeyan et al [13]. In a similar vein, increase in the Q < 0 as demonstrated graphically in Fig.5 and Fig.12 correspond to an increase in the temperature and velocity profiles of the nanofluid. The ϕ is one of the potent parameter that distinguishes nanofluids from other fluids. As displayed in Fig.6 and Fig.15, its increase brought about a corresponding decrease in the temperature and velocity profiles of the alumina nanofluid and when compared with the works of Polidori et al [10] and Mansour et al [11], the results followed similar trend. The Re examined the transition of nanofluids flow from laminar to turbulence. Fig.8 displayed the effect of numerical values of Re from laminar to turbulence and a corresponding increase in the velocity of the fluid was observed. The results is consistent with the works of Polidori et al [10], Mansour et al [11] and Ngiangia and Akazue [25] . The Gr is a determinant factor in natural convection and corresponds to cooling the plate (Gr > 0). Its effect, conducts heat away from the plates into the nanofluid and results in increasing the velocity of the nanofluid flow. Karthikeyan et al [13] and Ngiangia and Akazue [25] also reported the same findings. From Fig.13, it is shown that increase in the Ha which implies making the magnetic field strength within the region of the nanofluid stronger, diminishes the velocity profile. The study of the existence of magnetic field was also reported by Karthikeyan et al [13] and Ngiangia

and Akazue [25] and their findings are the same with this study. Finally, the χ as demonstrated in Fig.14, showed that increase in the χ, decreases the velocity of the nanofluid and the result is consistent with the works of Karthikeyan et al [13] and Ngiangia and Akazue [25].

Conclusion

Critically, a study of MHD alumina nanofluid through non-Darcian porous medium is made and findings show that the skin friction is not affected by the nanoparticle volume fraction while the magnetic Hartmann number, Reynolds number and porosity are not affected by the heat transfer coefficient. Generally, it is observed that the nanoparticle volume fraction is one of the most important parameters in the description of nanofluids and it decreases both the temperature and velocity profile of the alumina nanofluid. The comparison with the works of others which agree reasonably, also laid credence to the justification of the study.

References

[1]. Eckert, E.R.G and Drake, R.M. Heat and mass transfer, Tata McGraw-Hill, 2nd Ed., New Delhi, 1979.

[2] Raisinghania, M. D. Fluid dynamics (with hydrodynamics). S. Chand and Company LTD, New Delhi, 2003.

[3] Maiga, S. E. B., Nguyen, C. T., Galanis, N., and Roy, G. Heat transfer behaviours of nanofluids in a uniformly heated tube. Superlattices and Microstructures, 35, 543–557 (2004).

[4] Maiga, S. E. B., Nguyen, C. T., Galanis, N., and Roy,G. Hydrodynamic and thermal behaviours of a nanofluid in a uniformly heated tube. Volume 5 of Computational Studies, 453–462. WIT Press, (2004).

[5] Roy, G., Nguyen, C. T., and Lajoie, P.-R. Numerical investigation of laminar flow and heat transfer in a radial flow cooling system with the use of nanofluids. Super lattices and Microstructures, 35, 497–511 (2004).

[6] Wang, X.-Q., Mujumdar, A. S., and Yap, C. Free Convection Heat Transfer in Horizontal and Vertical Rectangular Cavities Filled with Nanofluids. In International Heat Transfer Conference IHTC-13. (2006).

[7] Khanafer, K., Vafai, K., and Lightstone, M. Bouyancy-driven heat transfer enhancement in a two-dimensional enclosure utilizing nanofluids. International Journal of Heat and Mass Transfer, 46, 3639–3653 (2003).

[8] Xuan, Y. and Roetzel, W. Conceptions for heat transfer correlation of nanofluids. International Journal of Heat and Mass Transfer, 43, 3701– 3707 (2000).

[9] Abu-Nada, E., Masoud, Z., Hijazi, A. Natural convection heat transfer enhancement in horizontal concentric annuli using nanofluids. International Communications in Heat and Mass Transfer, 35(5), 657–665 (2008).

[10] Polidori, G., Fohanno, S., and Nguyen, C. T. A note on heat transfer modeling of Newtonian nanofluids in laminar free convection. International Journal of Thermal Sciences, 46(8), 739–744 (2007).

[11] Mansour, R. B., Galanis, N., and Nguyen, C. T. Effect of uncertainties in physical properties on forced convection heat transfer with nanofluids. Applied Thermal Engineering, 27(1), 240–249 (2007).

[12] He, J H. Homotopy Perturbation Technique. Computational Methods Applications in Mechanical Engineering. 178: 257-262. (1999).

[13] Karthikeyan, S, Bhuvaneswari,M, Rajan, S and Sivasankaran, S. Thermal radiation effects on MHD convective flow over a plate in a porous medium by perturbation technique Applied Mathematics and Computational Intelligence. 2 (1) 75–83 (2013)

[14] Batchelor, G. The effect of Brownian motion on the bulk stress in a suspension of spherical particles. Journal of Fluid Mechanics, 83, 97–117 (1977).

[15] Bhattacharya, P., Saha, S. K., Yadav, A., Phelan, P. E., and Prasher, R. S. Brownian dynamics simulation to determine the effective thermal conductivity of nanofluids. Journal of Applied Physics, 95(11), 6492–6494 (2004).

[16] Tiwari, R. K and Das, M. K. Heat transfer augmentation in a two-sided lid-driven differentially heated square cavity utilizing nanofluids. International Journal of Heat and Mass Transfer. 50; 9-10. (2007).

[17] Asma, K; Khan, I and Sharidan, S. Exact solution for free convecton flow of nanofluids with ramped wall Temperature. The European Physical Journal-Plus. 130: 57-71. (2015),

[18] Aaiza, G; Khan I and Shafie S. Energy transfer in mixed convection mhd flow of nanofluid containing different shapes of nanoparticles in a channel filled with saturated porous medium. Nanoscle Research Letters. 10(490): 1-14. (2015).

[19] Cogley, A. C; Vincenti, A. W and Giles, E. S . Differential Approximation of a Radiative Heat Transfer. American Institute of Aeronautic and Astronautics Journal, 6: 551-553 (1968)

[20] Aruna, G, Varma, S V and Raju, R S Combined influence of Soret and Dufour effects on unsteady hydromagnetic mixed convective flow in an accelerated vertical wavy plate through a porous medium. International Journal of Advances in Applied Mathematics and Mechanics **3(1)** 122-134 (2015).

[21] Mebine, P. Radiation effects on MHD Couette flow with Heat transfer between two parallel plates. Global Journal of Pure and Applid Mathematics. 3(2): 191-202 (2007).

[22] He, J. H. Homotopy Perturbation Method: A new Nonlinear Analytical Technique. Application of Mathematical Computations. 135: 73-79. (2003).

[23] He, J. H. New Interpretation of Homotopy Perturbation Method. International Journal of Modern Physics B. 20: 2561-2568. (2006).

[24] Makinde, O. D and Mukutu, W. N. Hydromagnetic thermal boundary layer of nanofluids over a convectively heated flat plate with viscous dissipation and ohmic heating. U. P. B Science Bulletin Serie A. 76(2): 181-192. (2014).

[25] Ngiangia, A. T and Akaezue, N. N. Heat transfer of mixed convection electroconductivity flow of copper nanofluid with different shapes in a porous micro channel provoked by radiation and first order chemical reaction. Asian Journal of Physical and Chemical Sciences 7(1): 1-14, 2019.